

On the Zero-Bias Anomaly in Quantum Wires

S. Sarkozy,* F. Sfigakis,† K. Das Gupta, I. Farrer, D. A. Ritchie, G. A. C. Jones, and M. Pepper
Cavendish Laboratory, J. J. Thompson Avenue, Cambridge, CB3 0HE, United Kingdom

Undoped GaAs/AlGaAs heterostructures have been used to fabricate quantum wires in which the average impurity separation is greater than the device size. We compare the behavior of the Zero-Bias Anomaly against predictions from Kondo and spin polarization models. Both theories display shortcomings, the most dramatic of which are the linear electron-density dependence of the Zero-Bias Anomaly spin-splitting at fixed magnetic field B and the suppression of the Zeeman effect at pinch-off.

PACS numbers: 72.10.Fk, 72.25.Dc, 73.21.Hb, 73.23.Ad

Split gates [1] can be used to restrict transport from a two-dimensional electron gas (2DEG) to a ballistic one-dimensional (1D) channel. This results in the quantization of the differential conductance $G = dI/dV_{sd}$ in units of $G_0 = 2e^2/h$ at zero magnetic field [2, 3]. A shoulder on the riser of the first quantized plateau, the “0.7 anomaly” or “0.7 structure” [4], is not completely understood but generally acknowledged to result from electron-electron interactions. Although spin polarization models [5, 6, 7, 8, 9, 10] and 1D Kondo physics models [11, 12, 13] can describe many experiments, neither can explain all phenomena associated with the 0.7 structure. One example is the so-called zero-bias anomaly (ZBA): a peak in G centered at $V_{sd} = 0$ for $G < 2e^2/h$ when sweeping source-drain bias V_{sd} at a fixed gate voltage V_{gate} at low temperature T . Spin polarization models cannot alone predict its occurrence in quantum wires, although an embedded impurity near or in the 1D channel could produce a ZBA via the 0D Kondo effect [14, 15, 16, 17]. On the other hand, in 1D Kondo physics models, a bound state forms when $G < G_0$. In this context, a resonance observed by a non-invasive detector capacitively coupled to a quantum wire at threshold [18] as well as a triple-peaked structure in G at fixed V_{gate} below the 0.7 structure [19] are consistent with the presence of a localized state in 1D channels.

Systematically studying the ZBA in modulation-doped 2DEGs has proven difficult because of the large variability of its characteristics from device to device [20, 21], probably due to the randomly fluctuating background potential caused by the ionized dopants, significant even with the use of large (≥ 75 nm) spacer layers. This disorder is so pervasive that one can be led to wonder whether the ZBA always results from interactions between conduction electrons and a random localized state near the 1D channel. However, disorder can be dramatically reduced in undoped GaAs/AlGaAs heterostructures where an external electric field (via a voltage V_{top} on a metal top gate) electrostatically induces the 2DEG [22, 23]. Figure 1(a) shows the advantages of this technique, particularly at low carrier densities (see also Fig. 3 in Ref. [22]), a regime most relevant for the ZBA.

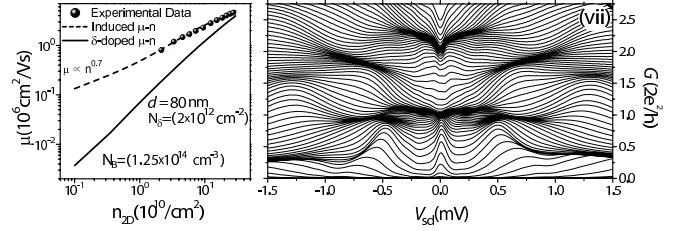


FIG. 1: (a) Measured (spheres) and calculated (dashed line) $\mu - n_{2D}$ relation for T622. For comparison, we simulate an otherwise identical 2DEG with a δ -doped layer 80 nm above. (b) G vs. V_{sd} incrementing V_{gate} (in steps of 0.3 mV) of a quantum wire in an undoped heterostructure ($T = 60$ mK). A ZBA can be observed in the riser of the $2e^2/h$ plateau.

In this Letter, we report on the study of the ZBA in ten quantum wires fabricated in undoped GaAs/AlGaAs heterostructures. We demonstrate that an unsplit ZBA does not result from interactions between conduction electrons and a random localized state near the 1D channel: it is a fundamental property of 1D channels, in disagreement with spin polarization models. Another inconsistency is a suppression of the Zeeman effect at pinch-off. In disagreement with Kondo theory, we observe a non-monotonic increase of the Kondo temperature T_K with V_{gate} , and a linear peak-splitting of the ZBA with V_{gate} at a fixed B .

The two wafers primarily used in this study, T622 (T623) with a 317 (117) nm deep 2DEG, were grown by molecular beam epitaxy and consisted of: a 17 nm GaAs cap, 300 (100) nm of $Al_{0.33}Ga_{0.67}As/GaAs$, 1 μm of GaAs, and a 1 μm superlattice with a 5 nm $Al_{0.33}Ga_{0.67}As/5$ nm GaAs period. No layer was intentionally doped. For T622, $n_{2D} = (0.275 V_{top}/V - 0.315) \times 10^{11} \text{ cm}^{-2}$. Figure 1(a) shows the mobility μ versus the 2D sheet carrier density n_{2D} for T622; wafer T623 has slightly higher mobilities, e.g. $1.7 \times 10^6 \text{ cm}^2/Vs$ versus $1.6 \times 10^6 \text{ cm}^2/Vs$ at $5 \times 10^{10} \text{ cm}^{-2}$. Using Matthiessen’s rule far from the localization regime, the experimental data is fit to standard models of scattering times $\frac{1}{\tau_{total}} = \sum_j \frac{1}{\tau_j}$ [24, 25]. The dominant sources of scattering in our system (analyzed in Ref. [23]) are charged background impurities and interface roughness, from which we extracted the background

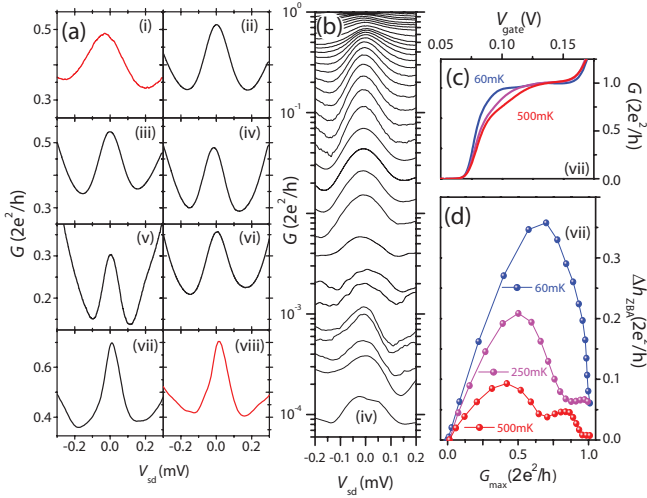


FIG. 2: (color online) (a) G vs. V_{sd} incrementing V_{gate} for eight quantum wires, labeled (i) through (viii). (b) For a wide range of G (on a log scale), the ZBA occurs far beyond the ballistic regime ($T \approx 150$ mK). (c) T dependence of the 0.7 structure at $V_{sd}=0$. (d) Δh_{ZBA} (defined in main text) for various T . A local minimum appears as T increases.

impurity concentration $N_B = 1.25 \times 10^{14} \text{ cm}^{-3}$. Intersecting the background impurity potential with a 2DEG wavefunction of width $\lambda \leq 20$ nm yields a minimum average distance between scattering centers $D = 0.6 \mu\text{m}$ in wafer T622. A similar number is found for wafer T623.

Ten quantum wires, labeled (i)–(x) throughout this paper (seven from T622 and three from T623), were measured in two dilution refrigerators (with base electron temperature 60 mK and ~ 150 mK), using standard lock-in techniques and varying T , B , V_{sd} , and n_{2D} . Following a mesa etch, recessed ohmic contacts (Ni/AuGe/Ni/Ti/Pt) were deposited and annealed [26]. A voltage V_{gate} can be applied to surface Ti/Au split gates of length $L = 400$ nm with width $W = 700$ (400) nm on on T622 (T623). Polyimide insulated the inducing Ti/Au top gate from other gates and ohmic contacts.

Although the average distance between impurities is $D \geq 0.6 \mu\text{m}$, their distribution is not uniform. In analogy to mean-free-path calculations, the probability P of finding an impurity within a 1D channel of length L is $P = 1 - e^{-(L/D)} \sim 50\%$. For $G \leq 0.8 G_0$, an unsplit, symmetric ZBA was observed in all ten devices. Figure 2(a) shows the ZBA in eight of these. It is thus unlikely (of order $\prod_{j=1}^{10} P_j \ll 1\%$) that *all* such occurrences were the result of interactions between conduction electrons and some localized state near the 1D channel.

Defining G_{max} as the maximum conductance achieved at base T , $V_{sd} = 0$, and $B = 0$ for each value of V_{gate} , Fig. 2(b) shows that G_{max} increases monotonically with V_{gate} (as in all our devices). Defining Δh_{ZBA} as G_{max} minus the average conductance of the local minima on the RHS and LHS of the ZBA, Fig. 2(d) shows that Δh_{ZBA}

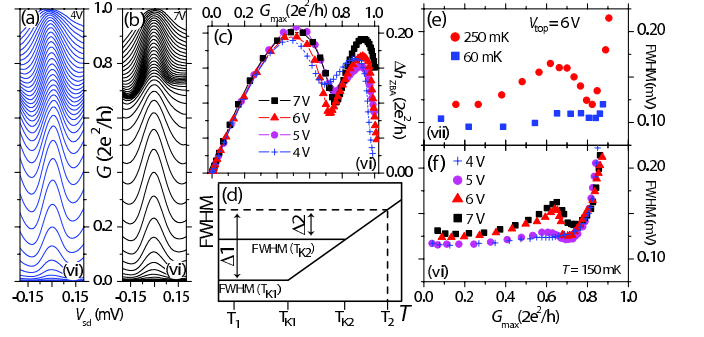


FIG. 3: (color online) G vs. V_{sd} incrementing V_{gate} ($T \approx 150$ mK) for: (a) $V_{top} = +4$ V ($n_{2D} = 0.8 \times 10^{11} \text{ cm}^{-2}$), and (b) $V_{top} = +7$ V ($n_{2D} = 1.6 \times 10^{11} \text{ cm}^{-2}$). (c) Δh_{ZBA} for $V_{top} = 4 - 7$ V. (d) Sketch showing $\text{FWHM} \propto \max[T, T_K]$ as T increases. (e) FWHM of the ZBA for $T = 60$ mK and 250 mK. (f) FWHM for $V_{top} = 4 - 7$ V from the dataset in panel (c).

decreases as T increases for all V_{gate} , as would be expected from Kondo physics. As T increases, a local minimum near $G_{max} \approx 0.75 G_0$ becomes more pronounced. In a previous study on doped quantum wires (see Fig. 6 in Ref. [19]), similar plots of Δh_{ZBA} also showed a local minimum near $G_{max} \approx 0.75 G_0$. Figure 2(c) links its appearance to the formation of the 0.7 structure.

Varying n_{2D} affects the Fermi energy of electrons entering the 1D channel from the 2D leads, as well as the 1D confinement potential [e.g. increasing $V_{top} = 4$ V in Fig. 3(a) to 7 V in Fig. 3(b), the energy-level spacing between the first two 1D subbands increases from 0.6 to 0.8 meV]. Figure 3(c) shows no clear trend for Δh_{ZBA} with increasing n_{2D} , but the minimum near $G_{max} \approx 0.75 G_0$ remains present in all curves. In the Kondo formalism [Fig. 3(d)], a specific T_K is associated with each V_{gate} , and the full width at half maximum (FWHM) of the ZBA should scale linearly either with its T_K if $T_K > T$, or with T if $T > T_K$ [16, 27]. For $G_{max} \geq 0.9 G_0$ in Fig. 3(f), we do not use the FWHM as it is difficult to distinguish the ZBA unambiguously from the bell-shape traces of G just below a plateau (see Fig. 6 in Ref. [28]). For $G_{max} < 0.7 G_0$ at $V_{top} = 4$ V, the FWHM remain essentially flat: $T > T_K$. For $0.5 G_0 < G_{max} < 0.7 G_0$, increasing n_{2D} appears to increase T_K beyond $T \approx 150$ mK. An upper limit of $T_K < \frac{\text{FWHM}}{k_B}$ at each V_{gate} can be estimated [17]. In most devices, regardless of whether the 0.7 structure is visible or not, the FWHM has a local minimum near $G_{max} \approx 0.75 G_0$. Identical minima are also observed in doped GaAs quantum wires (see Fig. 3 in Ref. [11]) and in GaN quantum wires (see Fig. 4 in Ref. [29]). Near $G_{max} \approx 0.75 G_0$, we interpret the FWHM minimum to indicate a suppression of Kondo interactions, leading to a non-monotonic increase of $T_K(V_{gate})$ from pinch-off to $2e^2/h$, in direct contradiction to 1D Kondo theory [12]. Kondo theory also predicts that $\text{FWHM}(T_{K1})$ will increase more than $\text{FWHM}(T_{K2})$ as T increases [i.e. $\Delta 1 > \Delta 2$ in

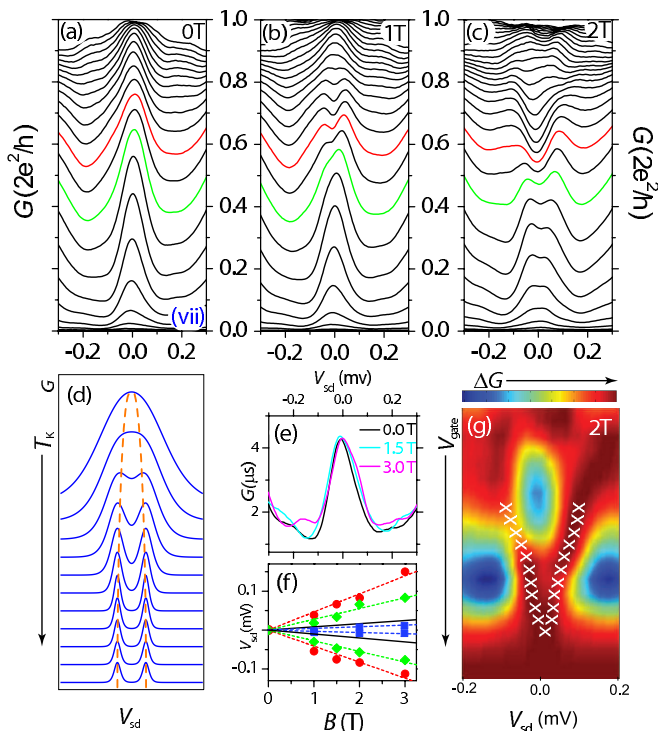


FIG. 4: (color) G vs. V_{sd} incrementing V_{gate} ($T = 60$ mK) for: (a) $B = 0$ T, (b) $B = 1$ T, and (c) $B = 2$ T. (d) Sketch of the expected splitting of the ZBA at constant B and T for the singlet Kondo effect as T_K alone is decreased from top to bottom (traces offset vertically). (e) Enlarged view of the ZBA being barely spin-split near pinch-off for device (vii). (f) Zeeman splitting of the ZBA as a function of B for the red and green traces in panels (a)–(c). The black solid line shows the expected peak-splitting $g\mu_B/e = 25 \mu\text{V}/T$ (for $|g| = 0.44$). The blue squares are from the data in panel (e). (g) Colorscale of the data from panel (c). The “x” symbols mark the location of the spin-split ZBA peaks.

Fig. 3(d)]. However, in further disagreement with theory, Fig. 3(e) shows the *opposite* behavior: the FWHMs associated with the larger Kondo temperatures increase the most.

Figures 4(a)–(c) show how the ZBA spin-splits at low B . At a fixed B , the peak-to-peak separation ΔV_{p-p} increases almost linearly with V_{gate} [Fig. 4(g)]. In an in-plane B , pinch-off voltage can change due to diamagnetic shift [30], making V_{gate} an unreliable marker. However, $G(|V_{sd}| > 0.25$ mV) is mostly insensitive to B , while the ZBA changes significantly. Thus, fitting the linear relation $\Delta V_{p-p} = \alpha B$ to the red points in Fig. 4(f), obtained from all red traces with $G = 0.65 G_0$ at $V_{sd} = 0.25$ mV in Figs. 4(a)–(c), yields $\alpha = (86 \pm 2) \mu\text{V}/T$. For all green traces with $G = 0.50 G_0$ at $V_{sd} = 0.25$ mV in Figs. 4(a)–(c), Fig. 4(f) yields $\alpha = (57 \pm 2) \mu\text{V}/T$. As V_{gate} decreases [from the red traces in Figs. 4(a)–(c) down to pinch-off], α appears to continuously decrease from $86 \mu\text{V}/T$ to small values [e.g. $\alpha < (16 \pm 5) \mu\text{V}/T$ from peak-fitting two

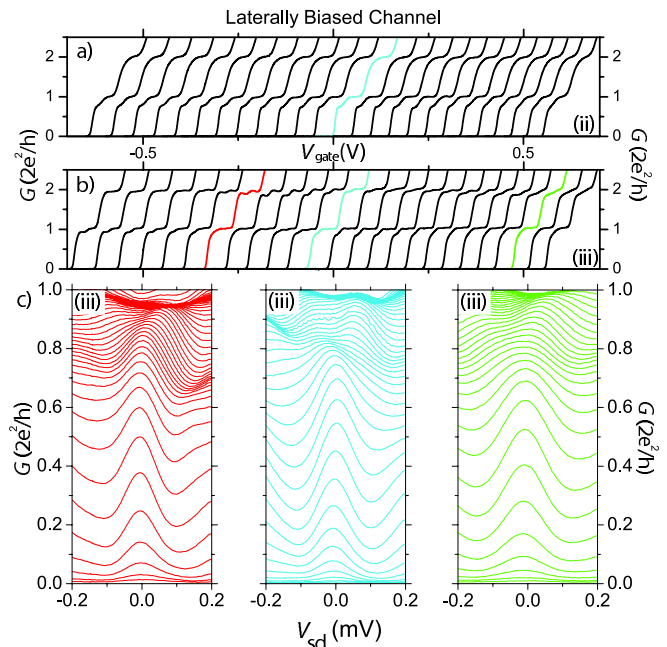


FIG. 5: (color) At $T \approx 150$ mK, a clean, “classic” 0.7 structure (a) can be distinguished from disorder effects (b) by laterally shifting the conducting 1D channel by differentially biasing the left and right gates by $\Delta V_g = V_{left} - V_{right}$ (traces offset laterally). Blue traces in both panels correspond to $\Delta V_g = 0$, and the leftmost (rightmost) trace to $\Delta V_g = +1.2$ V (-1.2 V). (c) G vs. V_{sd} incrementing V_{gate} corresponding to the red, blue, and green traces from panel (b). The apparent splitting at high G is related to disorder.

asymmetric gaussians to Fig. 4(e)].

At finite B , the ZBA in quantum dots splits into two peaks [16], whose peak-to-peak separation $e\Delta V_{p-p} = 2g^*\mu_B B$ is a defining characteristic of the Kondo effect [14] where μ_B is the Bohr magneton and g^* the effective Landé g factor. Figure 4(d) illustrates three distinct regimes one would expect from the singlet Kondo effect at fixed B and T [31, 32]. In the topmost traces, $k_B T_K > g^*\mu_B B > k_B T$: spin-splitting cannot be resolved. In the middle traces, $g^*\mu_B B > k_B T_K > k_B T$: the linewidth of each split peak is narrow enough to make the splitting visible. In the bottom traces, $g^*\mu_B B > k_B T > k_B T_K$: the split peaks shrink *but their splitting should remain constant* as long they are still resolvable. However, in our quantum wires, this is clearly not the case. The variation of $\Delta V_{p-p} = \alpha B$ with V_{gate} in Fig. 4(b)–(c) cannot be reconciled with singlet Kondo physics.

In quantum dots, the ZBA splitting can vary with V_{gate} for $B \geq 0$ (Fig. 4 in Ref. [33], Fig. 3 in Ref. [34]) from the competition between the Kondo effect and the Ruderman-Kittel-Kasuya-Yosida (RKKY) interaction between two localized spins [35]. Although two such localised spins are predicted to form in quantum wires near pinch-off [10, 13] and these could explain the behavior observed in Figs. 4(b)–(c), this scenario would also

require the ZBA to be split at $B = 0$. This is not the case [Figs. 2(b), 3(a)–(b), 4(a), 5(c)]: the two-impurity Kondo model is not applicable.

In spin-polarization models [5, 6, 7, 8, 9, 10], the energy difference between spin-up and spin-down electrons $\Delta E_{\uparrow\downarrow} = g\mu_B B + E_{\text{ex}}(n_{1\text{D}})$ includes E_{ex} , an exchange-enhanced spin splitting that could account for previous observations of an enhanced g factor above the value $|g| = 0.44$ of bulk GaAs [4]. Neglecting correlation effects, the bare exchange energy in 1D scales linearly with $n_{1\text{D}}$. Assuming $n_{1\text{D}} \propto V_{\text{gate}}$, the almost linear splitting of the ZBA is consistent with a density-dependent spin polarization. However, this scenario would also require that the minimum value of $e\alpha$ be the bare Zeeman energy $g\mu_B = 25 \mu\text{eV/T}$. This is not what we observe: $e\alpha < 16 \mu\text{eV/T}$ in Fig. 4(e). Instead, we find $\Delta E_{\uparrow\downarrow} = g^*(n_{1\text{D}})\mu_B B$, where $0.27 < g^*(n_{1\text{D}}) < 1.5$ [Fig. 4(f)]. The Zeeman effect can be suppressed ($g^* \sim 0.2$) if a 2DEG significantly penetrates into the AlGaAs barriers [36], at high $n_{2\text{D}}$ or if the 2DEG is close to the surface. Neither situation applies to our devices. The suppression of the bare Zeeman effect at pinch-off in our quantum wires is not consistent with spin polarization models.

Despite their exceptional device-to-device reproducibility (compared with doped wires), undoped quantum wires are not free from disorder [Fig. 5(b)]. The apparent splitting for $G \geq 0.8 G_0$ in some of our devices [Fig. 5(c)] is not due to spontaneous spin-splitting or RKKY vs. Kondo interactions, but rather to resonant backscattering or length resonances [37]. By increasing the 2D density (and thus long-range screening), many disorder-related effects can be minimized.

In summary, we provide compelling evidence for the ZBA to be a fundamental property of quantum wires. Its continued presence from $G \sim 2e^2/h$ down to $G \sim (2e^2/h) \times 10^{-5}$ suggests it is a different phenomenon to the 0.7 structure, as proposed in [18, 19]. Both 1D Kondo physics and spin polarization models fall short of accurately predicting experimental observations. For 1D Kondo physics models, these are: (i) a non-monotonic increase of T_K with V_{gate} , (ii) the FWHM of the ZBA not scaling with $\max[T, T_K]$ as T increases, and (iii) a linear peak-splitting of the ZBA with V_{gate} at fixed B . Spin polarization models can account neither for the occurrence of the ZBA nor for the suppression of the bare Zeeman effect at pinch-off. It is hoped that further refinements in theory will account for these observations.

The authors acknowledge D. Anderson, H. Quach and C. Namba for electron beam patterning, and V. Tripathi, K.-F. Berggren, A.R. Hamilton, C.J.B. Ford, J.P. Griffiths, T.M. Chen, K.J. Thomas, and N.R. Cooper for useful discussions. S. Sarkozy acknowledges financial support as a Northrop Grumman Space Technology Doc-

toral Fellow. I. Farrer thanks Toshiba Research Europe for financial support.

-
- * On leave from Northrop Grumman Space Technology, One Space Park, Redondo Beach, California, 90278; e-mail: stephen.sarkozy@ngc.com
- † e-mail: fs228@cam.ac.uk
- [1] T. J. Thornton, M. Pepper, H. Ahmed, D. Andrews, and G. J. Davies, *Phys. Rev. Lett.* **56**, 1198 (1986).
 - [2] B. J. van Wees *et al.*, *Phys. Rev. Lett.* **60**, 848 (1988).
 - [3] D. A. Wharam *et al.*, *J. Phys. C* **21**, L209 (1988).
 - [4] K. J. Thomas *et al.*, *Phys. Rev. Lett.* **77**, 135 (1996).
 - [5] C. K. Wang and K. F. Berggren, *Phys. Rev. B* **54**, R14257 (1996).
 - [6] A. Kristensen *et al.*, *Phys. Rev. B* **62**, 10950 (2000).
 - [7] D. J. Reilly *et al.*, *Phys. Rev. Lett.* **89**, 246801 (2002).
 - [8] A. C. Graham, D. L. Sawkey, M. Pepper, M. Y. Simmons, and D. A. Ritchie, *Phys. Rev. B* **75**, 035331 (2007).
 - [9] F. Sfigakis *et al.*, *J. Phys.: Condens. Matter* **20**, 164213 (2008).
 - [10] K. F. Berggren and I. Yakimenko, *J. Phys.: Condens. Matter* **20**, 164203 (2008).
 - [11] S. Cronenwett *et al.*, *Phys. Rev. Lett.* **88**, 226805 (2002).
 - [12] Y. Meir, K. Hirose, and N. S. Wingreen, *Phys. Rev. Lett.* **89**, 196802 (2002).
 - [13] T. Rejec and Y. Meir, *Nature* **442**, 900 (2006).
 - [14] Y. Meir, N. S. Wingreen, and P. A. Lee, *Phys. Rev. Lett.* **70**, 2601 (1993).
 - [15] D. Goldhaber-Gordon *et al.*, *Nature* **391**, 156 (1998).
 - [16] S. M. Cronenwett *et al.*, *Science* **281**, 540 (1998).
 - [17] W. G. van der Wiel *et al.*, *Science* **289**, 2105 (2000).
 - [18] Y. Yoon *et al.*, *Phys. Rev. Lett.* **99**, 136805 (2007).
 - [19] F. Sfigakis *et al.*, *Phys. Rev. Lett.* **100**, 026807 (2008).
 - [20] A. C. Graham *et al.*, submitted to *Phys. Rev. B* (2008).
 - [21] J. P. Griffiths (unpublished).
 - [22] R. H. Harrell *et al.*, *Appl. Phys. Lett.* **74**, 2328 (1999).
 - [23] S. Sarkozy *et al.*, submitted to *Appl. Phys. Lett.* (2008).
 - [24] T. Ando, A. B. Fowler, and F. Stern, *Rev. Mod. Phys.* **54**, 437 (1982).
 - [25] A. Gold, *Phys. Rev. B* **38**, 10798 (1988).
 - [26] S. Sarkozy *et al.*, *Electrochemical Soc Proc.* **11**, 75 (2007).
 - [27] L. Glazman and M. Raikh, *JETP Letters* **47**, 452 (1988).
 - [28] L. Martin-Moreno, J. T. Nicholls, N. K. Patel, and M. Pepper, *J. Phys.: Condens. Matter* **4**, 1323 (1992).
 - [29] H. T. Chou *et al.*, *Appl. Phys. Lett.* **86**, 073108 (2005).
 - [30] F. Stern, *Phys. Rev. Lett.* **21**, 1687 (1968).
 - [31] M. Pustilnik and L. I. Glazman, *J. Phys.: Condens. Matter* **16**, R513 (2004).
 - [32] R. M. Potok *et al.*, *Nature* **446**, 167 (2007).
 - [33] H. Jeong, A. M. Chang, and M. R. Melloch, *Science* **293**, 2221 (2001).
 - [34] J. C. Chen, A. M. Chang, and M. R. Melloch, *Phys. Rev. Lett.* **92**, 176801 (2004).
 - [35] L. G. G. V. Dias da Silva, N. P. Sandler, K. Ingersent, and S. E. Ulloa, *Phys. Rev. Lett.* **97**, 096603 (2006).
 - [36] A. Kogan *et al.*, *Phys. Rev. Lett.* **93**, 166602 (2004).
 - [37] P. E. Lindelof and M. Aagesen, *J. Phys.: Condens. Matter* **20**, 164207 (2008).